



Published in final edited form as:

Med Sci Sports Exerc. 2022 December 01; 54(12): 2020–2030. doi:10.1249/MSS.0000000000003016.

Enhanced Bone Size, Microarchitecture, and Strength in Female Runners with a History of Playing Multidirectional Sports

Stuart J. Warden^{1,2,3}, Austin M. Sventeckis¹, Rachel K. Surowiec^{2,4}, Robyn K. Fuchs^{1,2}

¹Department of Physical Therapy, School of Health and Human Sciences, Indiana University, Indianapolis;

²Indiana Center for Musculoskeletal Health, Indiana University, Indianapolis;

³La Trobe Sport and Exercise Medicine Research Centre, La Trobe University, Bundoora, Victoria, AUSTRALIA;

⁴Department of Biomedical Engineering, Purdue School of Engineering and Technology, Indiana University-Purdue University Indianapolis, Indianapolis

Abstract

Purpose: Female runners have high rates of bone stress injuries (BSIs), including stress reactions and fractures. The current study explored multidirectional sports (MDS) played when younger as a potential means of building stronger bones to reduce BSI risk in these athletes.

Methods: Female collegiate-level cross-country runners were recruited into groups: 1) RUN: history of training and/or competing in cross-country, recreational running/jogging, swimming and/or cycling only and 2) RUN+MDS: additional prior history of training and/or competing in soccer or basketball. High-resolution peripheral quantitative computed tomography was used to assess the distal tibia, common BSI sites (diaphysis of the tibia, fibula and 2nd metatarsal), and high-risk BSI sites (base of the 2nd metatarsal, navicular and proximal diaphysis of the 5th metatarsal). Scans of the radius were used as control sites.

Results: At the distal tibia, RUN+MDS (n=18) had enhanced cortical area (+17.1%) and thickness (+15.8%) and greater trabecular bone volume fraction (+14.6%) and thickness (+8.3%) compared to RUN (n=14) (all $p < 0.005$). Failure load was 19.5% higher in RUN+MDS ($p < 0.001$). The fibula diaphysis in RUN+MDS had 11.6% greater total area and 11.1% greater failure load (all $p < 0.03$). At the 2nd metatarsal diaphysis, total area in RUN+MDS was 10.4% larger with greater cortical area and thickness and 18.6% greater failure load (all $p < 0.05$). RUN+MDS had greater trabecular thickness at the base of the 2nd metatarsal and navicular and greater cortical area and thickness at the proximal diaphysis of the 5th metatarsal (all $p < 0.02$). No differences were observed at the tibial diaphysis or radius.

Address for Correspondence: Stuart J. Warden, Department of Physical Therapy, School of Health and Human Sciences, Indiana University, 1140 W. Michigan St., CF-120, Indianapolis, IN 46202; stwarden@iu.edu.

Author contributions

S.J.W. and R.K.F. contributed to study design; all authors contributed to the acquisition, analysis and interpretation of data; S.J.W. drafted the paper; all authors critically revised the paper and approve of its final version.

Conclusion: These findings support recommendations that athletes delay specialization in running and play MDS when younger to build a more robust skeleton and potentially prevent BSIs.

Keywords

EXERCISE; PHYSICAL ACTIVITY; RELATIVE ENERGY DEFICIENCY IN SPORT; RUNNING; STRESS FRACTURE; STRESS REACTION

INTRODUCTION

Bone stress injuries (BSIs), including stress reactions and stress fractures, are believed to develop as a result of mechanical fatigue wherein repetitive loading below yield levels results in microdamage formation (1). Microdamage is a normal phenomenon that leads to skeletal renewal via targeted remodeling (2). However, suboptimal workload (e.g., too rapid progression of loading) can promote microdamage accumulation, coalescence, and/or extension leading to BSI development (3).

Microdamage forms in response to the interaction between the number of times a bone is loaded and the magnitude and rate of the tissue stresses and strains engendered. The relationship can be described by an inverse power law which indicates that small decreases in stress and strain dramatically increases the number of cycles until fatigue failure. For example, for loads relevant to running, it has been estimated that a 10% decrease in tissue stress and strain results in a doubling of the number of loading cycles before fatigue failure (4).

One way to reduce tissue stresses and strains for a given applied load is to have stronger bones. Stronger bones may be developed via mechanically-induced bone adaptation. Using professional baseball players as a within-subject controlled model, we demonstrated that humeral diaphysis adaptation to throwing-related loading nearly doubled bone strength to maintain tissue strains below injury thresholds (5). Using a within-subject controlled animal model, we found moderate (<10%) loading induced gains in bone mass generated an exponential (>100-fold) gain in bone fatigue resistance as a result of less tissue level strain during each loading cycle (6).

Playing multidirectional sports (MDS) when young may build a more robust skeleton to reduce BSI risk. Studies in both athletic and military populations have observed that individuals with a history of playing ball sports have lower BSI risk (7–9). The hypothesized mechanism is the development of a stronger skeleton (10). Ball sports, like basketball and soccer, introduce multidirectional loads to engender high-magnitude strains and strain rates in different bone regions (11). Basketball and soccer players exhibit enhanced skeletal properties (12, 13) and experience lower bone strains during loading than runners and controls (14, 15).

Female cross-country athletes have the highest rates of BSIs (16, 17). Poor bone health may be a factor. Up to 40% of female adolescent cross-country runners have a z score below –1 for spine areal bone mineral density (aBMD) (18). Insufficient caloric intake to meet energy

demands (i.e. Relative Energy Deficiency in Sport [RED-S]) contributes in some athletes. However, a focus on running activities when younger, at the expense of participating in other sports, may also play a role. Female high school distance runners who highly specialized in distance running (running >9 mth/yr with no participation in other sports) were found to have lower spine aBMD than those who did not specialize (19).

To explore whether playing ball sports when younger enhances bone properties in female cross-country runners, the current study compared collegiate-level runners who participated in MDS around the pubertal period to runners who solely ran (and swam or cycled). The study principally utilized high-resolution peripheral quantitative computed tomography (HR-pQCT) to assess bone properties at the distal tibia and common BSI sites (diaphysis of the tibia, fibula and 2nd metatarsal [MT]). Bone properties were also assessed at select high-risk BSI sites (base of the 2nd MT, navicular and proximal diaphysis of the 5th MT). BSIs at the latter sites are considered high risk as injuries at those locations are prone to delayed or nonunion and/or are at high risk of progression to complete fracture (20).

METHODS

Participants

A convenience sample of non-pregnant females aged 18 years were recruited. They were current members of a Division I or II cross-country team within the National Collegiate Athletic Association (NCAA), but could also compete in track events 1,500 m. Shorter events potentially alter lower extremity loading distribution, with power (sprinters, jumpers, hurdlers) and endurance (middle distance and distance runners) athletes having relatively higher incidences of foot and leg BSIs, respectively (21).

The study was approved by the Institutional Review Board of Indiana University and written informed consent was obtained. Potential participants completed a screening questionnaire for self-reported historical participation in different sports. For activities they had trained and/or competed in more than twice per month for 4 months per year, they were asked what age/s they participated and how many times per month and how many months per year they participated.

Participants were eligible for the running group (RUN group) if they reported a history of training and/or competing only in cross-country, recreational running/jogging, swimming and/or cycling. Participants were eligible for the running and MDS group (RUN+MDS group) if they also had a history of training and/or competing in either soccer or basketball twice or more per week for at least 6 months per year for 5 years beginning prior to 10 years of age. These criteria were to encourage: 1) MDS being performed over the adolescent growth period—the window considered prime for bone mechanoadaptation and 2) exposure to a sufficient frequency and duration of MDS.

Exclusion criteria for both groups were: 1) history of participating in gymnastics more than twice per month for 4 months per year for more than 2 years, as the non-dominant radius was used as a control site and gymnasts have bilaterally enhanced radial bone health (22); 2) a history of a BSI or fracture on both sides of the body in any of the bones to be imaged;

3) lower extremity surgery or immobilization for >2 weeks within the past 2 years, and 4) known metabolic bone disease or systemic condition known to influence bone health.

Participant characteristics

Height and weight were measured and BSI history (including number and location/s), age of menarche, and best cross-country 5 km time were self-reported. The Low Energy Availability in Females Questionnaire (LEAF-Q) was used to identify physiological symptoms of low energy availability (including gastrointestinal and menstrual function), with a score ≥ 8 indicating elevated risk (23). Appendicular skeletal muscle mass relative to height ($ASM/height^2$; kg/m^2) and whole-body aBMD were measured by whole-body dual-energy x-ray absorptiometry (DXA) (Norland Elite; Norland at Swissray, Fort Atkinson, WI). Regional DXA scans assessed total hip and spine aBMD.

High-resolution peripheral quantitative computed tomography (HR-pQCT)

A HR-pQCT scanner (XtremeCT II; Scanco Medical, Bruttisellen, Switzerland) operating at 68 kVp and 1.47 mA with a voxel size of 60.7 μm was used to image the radius, tibia/fibula, MTs and navicular (Fig. 1). Scans were performed of the participants' non-dominant arm and ipsilateral leg. The contralateral side was imaged in individuals with a history of a BSI or fracture in the bone to be imaged. Participants laid supine with the segment to be imaged immobilized using a padded carbon fiber cast provided by the scanner manufacturer. The casts were anatomically formed to the arm and leg. MTs and navicular scans were achieved by plantarflexing the foot onto the leg cast with a wedge placed under the forefoot to position the 2nd MT parallel to the scanner's z-axis. The hip and knee were positioned in flexion to reduce stress on the anterior ankle but allow the gantry door of the scanner to be lowered. Elastic straps around the lower leg and foot were used for stabilization and bolsters placed under the thigh and leg to provide support.

Scans taking 168 slices (10.2 mm of bone length) of radial and tibial sites were acquired as previously described (24). Reference lines were placed at the medial edge of the distal radius articular surface and center of the tibia joint surface. Scan stacks were centered 4% (distal radius) and 30% (radial diaphysis) of bone length proximal to the radius reference line and 7.3% (distal tibia) and 30% (tibial diaphysis) of bone length proximal to the tibia reference line. Bone length was measured in triplicate before scanning using a segmometer (Realmet Flexible Segmometer, NutriActiva, Minneapolis, MN). Outcomes for the fibula diaphysis were acquired from the scans performed at the tibial diaphysis scan location.

Multi-stack scans were used to image the MTs and navicular. Up to nine stacks (each stack consisting of 168 slices or 10.2 mm of bone length) were used to image all 5 MTs. A reference line was placed distal to the head of the 2nd MT (most distal MT region) and stacks imaged proximally until beyond the styloid process of the 5th MT (most proximal MT region). For the navicular, three scan stacks imaged proximal from a reference line positioned at the navicular-cuneiform joint. All scans were scored for motion artifacts on a standard scale of 1 (no motion) to 5 (significant blurring of the periosteal surface, discontinuities in the cortical shell). No scans scored >3 .

Reconstructed images of the distal radius and tibia, and diaphysis of the radius, tibia, fibula, 2nd MT and proximal 5th MT were analyzed according to the manufacturer's standard protocol. The outer periosteal surface was semi-automatically contoured and the inner endosteal surface identified using the manufacturer's automatically generated endocortical contour. Images were filtered with a low-pass Gaussian filter (sigma 0.8, support 1.0 voxel) and fixed thresholds used to extract trabecular and cortical bone (320 and 450 mgHA/cm³, respectively).

For the 2nd MT diaphysis, 168 slices (10.2 mm of bone length) spanning the midshaft of the bone were analyzed. Bone length was measured as the distance between the most proximal and distal slices containing the 2nd MT base and head, respectively. For the proximal 5th MT, bone length was determined from the most distal and proximal slices containing the MT head and styloid process, respectively. One hundred slices (6.1 mm of bone length) were analyzed beginning one-third of 5th MT bone length distal to the tip of the styloid process (Fig. 1F). This region is distal to the articulation between the 4th and 5th MTs and in Zone III of the 5th MT where BSIs occur (25).

The following outcomes were measured at the distal radius and tibia (trabecular bone rich sites with a cortical shell): total volumetric BMD (Tt.vBMD, mgHA/cm³) and area (Tt.Ar, mm²); cortical vBMD (Ct.vBMD, mgHA/cm³), area (Ct.Ar, mm²), and thickness (Ct.Th, mm); and trabecular vBMD (Tb.vBMD, mgHA/cm³), area (Tb.Ar, mm²), bone volume/total volume (Tb.BV/TV, %), thickness (Tb.Th, mm), number (Tb.N, 1/mm), and separation (mm).

The following outcomes were measured at the radial, tibial, fibular, 2nd MT and proximal 5th MT diaphysis (cortical bone predominant sites): Ct.vBMD (mgHA/cm³), Tt.Ar (mm²), Ct.Ar (mm²), Ct.Th (mm), cortical porosity (Ct.Po, %), and minimum (I_{MIN} , cm⁴), maximum (I_{MAX} , cm⁴) and polar (I_p , cm⁴) moment of inertias. Diaphyseal robustness was calculated as Tt.Ar divided by bone length (26), with bone length measured as described earlier. Fibula length was not measured so tibia length was used as a surrogate.

Micro-finite element analysis (Scanco Medical FE software version 1.13) was used to estimate failure load (kN) at the radial and tibial sites and the fibula and 2nd MT diaphyses. Each voxel within the segmented images was assigned a modulus of 10 GPa and Poisson's ratio of 0.3. Axial compression was applied and failure load estimated when 5% of elements exceeded 1% strain (27). In addition to raw values, cortical, trabecular and failure load outcomes at radial and tibial sites were expressed as z scores relative to reference data obtained using the same HR-pQCT scanner (28).

Analyses at the base of the 2nd MT and navicular were limited to trabecular outcomes due to limited cortical bone at these locations. For the base of the 2nd MT, 100 slices (6.1 mm of bone length) were analyzed beginning 5% of bone length from the most proximal slice containing the 2nd MT. Navicular outcomes were obtained by analyzing 100 slices (6.1 mm of bone length) mid-way between the floor of the facet that articulates with the talus head and the most distal navicular portion at the navicular-cuneiform complex. At both the base of the 2nd MT and navicular, a region of interest was manually traced inside

the outer boundary of the bone every 10 slices (Fig. 1D, E). The region was morphed on intervening slices and visually inspected. Images were filtered (sigma 0.8, support 1.0 voxel) and trabecular bone extracted (threshold = 320 mgHA/cm³) to acquire Tb.BV/TV, Tb.Th, Th.N and Tb.Sp.

Short-term precision on duplicate tibial (including fibula) and radial scans with repositioning in 15 individuals showed root mean square coefficients of variation (RMS-CV) of <0.6% for bone density (Tt.vBMD, Ct.vBMD, Tb.vBMD) and <0.8% for bone size (Tt.Ar, Ct.Ar, Tb.Ar) at both distal and diaphyseal sites, and 1.8–2.9% and <1% for estimated failure load at distal and diaphyseal sites, respectively. RMS-CVs for trabecular microarchitecture outcomes (Tb.BV/TV, Tb.N, Tb.Th, Tb.Sp) at distal sites were 0.7–3.2%. Short-term precision for outcomes at MT and navicular sites is currently not available.

Statistical analyses

Two-tailed analyses with $\alpha=0.05$ were performed with IBM SPSS Statistics (v28; IBM Corporation, Armonk, NY). Participant demographics were compared between RUN and RUN+MDS using unpaired t-tests (ratio data) or Chi-squared tests (nominal data). Univariate general linear model analyses compared DXA and HR-pQCT outcomes between groups. LEAF-Q score and whole-body lean mass were included as covariates in group comparisons of DXA and trabecular HR-pQCT (Tb.BV/TV, Tb.N, Tb.Th, Tb.Sp) outcomes. In addition to LEAF-Q score and whole-body lean mass, bone length was included as a covariate in analyses of HR-pQCT measures of bone size (Tt.Ar, Ct.Ar, Tb.Ar, Ct.Th) and strength (I_{MIN} , I_{MAX} , I_p , failure load).

RESULTS

Participant characteristics

Fourteen and 18 participants were recruited into the RUN and RUN+MDS groups, respectively. The groups were comparable for age, age of menarche, LEAF-Q score, present and historical menstrual function (acquired from the LEAF-Q), age started and total years competing in cross-country, and best cross-country performance (all $p=0.38-0.99$) (Table 1). There was an equal frequency of participants at risk of low energy availability (LEAF-Q score = 8) in each group ($p=0.53$). There were no differences between groups for BSI history ($p=0.26$) or the number of BSIs per athlete ($p=0.14$). The RUN+MDS group played soccer ($n=7$), basketball ($n=6$) or both ($n=5$) for 10.3 ± 3.2 yrs (range = 5–14 yrs) beginning 7.7 ± 2.4 yrs prior to menarche (range = 5–11 yrs) and finishing at 16.1 ± 2.5 yrs of age (range = 12–19 yrs).

RUN and RUN+MDS were comparable for height, weight, BMI, and whole-body lean and percent fat mass (all $p=0.09-0.84$) (Table 1). DXA-derived whole-body and lumbar spine aBMD were 5.8% and 8.0% higher in RUN+MDS than RUN, respectively (all $p < 0.05$). There were no differences between groups for hip areal BMD ($p=0.31$). aBMD was below reference values (z score < 0) at the lumbar spine in the RUN group and above reference values (z score > 0) at the hip in both the RUN and RUN+MDS groups.

There were no group differences for HR-pQCT outcomes at the distal radius (see Supplemental Fig. 1, Distal radius properties in RUN and RUN+MDS, SDC 1) or radial diaphysis (see Supplemental Fig. 2, HRpQCT properties of the radial diaphysis in RUN and RUN+MDS, SDC 2) (all $p=0.10$ to 0.98). Distal radius and radial diaphysis outcomes in both RUN and RUN+MDS did not differ from reference values, except for lower Ct.Ar and failure load in RUN and higher Ct.vBMD in RUN+MDS at the radial diaphysis (see Supplemental Fig. 3A,B, Z scores for HRpQCT properties of the distal radius, radial diaphysis, distal tibia, and tibial diaphysis in RUN and RUN+MDS, SDC 3).

Distal tibia

RUN+MDS had 12.4% greater Tt.vBMD at the distal tibia compared to RUN ($p<0.01$) (Fig. 2A) with 15.9% greater Tb.vBMD ($p<0.01$) (Fig. 2C). There were no differences between groups for Ct.vBMD ($p=0.74$) (Fig. 2B). Overall size (Tt.Ar) of the distal tibia was the same between groups ($p=0.41$) (Fig. 2D), but RUN+MDS had 17.1% greater Ct.Ar ($p=0.002$) (Fig. 2E) and 15.8% greater Ct.Th ($p=0.015$) (Fig. 2G) than RUN. RUN+MDS had 14.6% greater Tb.BV/TV ($p=0.005$) (Fig. 2H) with 8.3% greater Tb.Th ($p=0.005$) (Fig. 2I). There were no differences between RUN and RUN+MDS for Tb.N or Tb.Sp (all $p=0.53$ – 0.63) (Fig. 2J, K). Failure load at the distal tibia was 19.5% higher in RUN+MDS compared to RUN ($p<0.001$) (Fig. 2L).

HR-pQCT outcomes at the distal tibia in RUN were equivalent to reference values for all outcomes, except Tt.Ar (z score = -0.52 ; 95% confidence interval [CI] = -1.01 to -0.04) (see Supplemental Fig. 3C, Z scores for HRpQCT properties of the distal radius, radial diaphysis, distal tibia, and tibial diaphysis in RUN and RUN+MDS, SDC 3). RUN+MDS had elevated distal tibia HR-pQCT outcomes compared to reference values for Tt.vBMD, Tb.vBMD, Ct.Ar, Ct.Th, Tb.BV/TV and Tb.Th. The z score for failure load at the distal tibia in the RUN+MDS group was $+0.80$ (95% CI = $+0.43$ to $+1.16$).

Tibial diaphysis

There were no differences in any HR-pQCT measures at the tibial diaphysis between RUN and RUN+MDS (all $p=0.42$ – 0.94) (see Supplemental Fig. 4, HRpQCT properties of the tibial diaphysis in RUN and RUN+MDS, SDC 4). HR-pQCT outcomes at the tibial diaphysis were equivalent to reference values for all outcomes, except for Ct.Th in both RUN (z score = $+0.91$; 95% CI = $+0.51$ to $+1.31$) and RUN+MDS (z score = $+0.89$; 95% CI = $+0.45$ to $+1.32$) (see Supplemental Fig. 3D, Z scores for HRpQCT properties of the distal radius, radial diaphysis, distal tibia, and tibial diaphysis in RUN and RUN+MDS, SDC 3).

Fibula diaphysis

The fibula diaphysis in RUN+MDS was 11.6% larger (Tt.Ar) with 12.0% more Ct.Ar compared to RUN (all $p<0.03$) (Fig. 3B, C). I_{MIN} at the fibula diaphysis was 28.5% greater in RUN+MDS compared to RUN ($p=0.02$) (Fig. 3F), but significance was not reached for I_{MAX} or I_p (all $p=0.06$ – 0.13) (Fig. 3G, H). There were no differences between RUN and RUN+MDS for Ct.vBMD, Ct.Th or Ct.Po at the fibula diaphysis (all $p=0.22$ – 0.95 ; Fig. 3A, D, E). The fibula diaphysis in RUN+MDS was 8.4% and 11.1% more robust and stronger than in RUN, respectively (all $p < 0.03$) (Fig. 3I, J).

Second metatarsal (2nd MT) diaphysis

Tt.Ar of the 2nd MT in RUN+MDS was 10.4% larger compared to RUN with 18.7% and 19.9% greater Ct.Ar and Ct.Th, respectively (all $p < 0.05$) (Fig. 4A, C, D). I_{MAX} and I_p at the 2nd MT diaphysis were 32.5% and 23.3% greater in RUN+MDS compared to RUN, respectively (all $p < 0.04$) (Fig. 4H & I). There were no differences between RUN and RUN+MDS for Ct.vBMD, Ct.Po or I_{MIN} at the 2nd MT diaphysis (all $p = 0.40-0.86$) (Fig. 4A, E, F, G). The 2nd MT diaphysis in RUN+MDS was 9.2% and 18.6% more robust and stronger than in RUN, respectively (all $p < 0.04$) (Fig. 4I, J).

High risk BSI sites

RUN+MDS had 5.3% and 10.1% greater Tb.Th compared to RUN at the base of the 2nd MT and navicular, respectively (all $p < 0.02$) (Table 2). The greater Tb.Th at the navicular contributed to 8.9% higher Tb.BV/TV in RUN+MDS compared to RUN ($p = 0.01$). The proximal diaphysis of the 5th MT in RUN+MDS had 10.9% and 11.6% greater Ct.Ar and Ct.Th than in RUN, respectively (all $p < 0.02$). There were no group differences in I_{MIN} , I_{MAX} or I_p at the proximal diaphysis of the 5th MT (all $p = 0.06-0.09$).

DISCUSSION

The current findings support recommendations that runners participate in ball sports when younger to promote skeletal development and potentially prevent BSIs (3, 10, 29). Female collegiate level cross-country runners who participated in MDS (soccer, basketball or both) before and across their pubertal growth period had enhanced bone microarchitecture and greater strength at their distal tibia and enhanced bone size and strength at the diaphysis of their fibula and 2nd MT compared to runners who solely ran (and did low impact sports). The strength enhancements ranged from an average of 11.1% at the fibula diaphysis to 19.5% at the distal tibia. In those who played MDS, there were also enhancements in bone microarchitecture at high-risk BSI sites, namely the base of the 2nd MT, navicular and proximal diaphysis of the 5th MT. There was no benefit of MDS on properties of the tibial diaphysis.

Previous studies in both military and athlete populations reported prior participation in ball sports reduced BSI risk (7–9). In over 1,000 recruits, Milgrom and colleagues (8) observed that playing MDS (principally basketball) for at least 2 years prior to infantry basic training reduced the risk of BSI by over half. Similarly, Fredericson and colleagues (7) reported that playing soccer or basketball reduced BSI risk by nearly half in 274 elite runners. The hypothesis in both studies was that ball sports enhanced skeletal health, but this theory was not tested. Most recently, Rudolph et al. (30) reported that women who spent a greater proportion of their time playing MDS had a lower risk of multiple BSIs. We did not find a difference in BSI history between groups, likely due to our low participant numbers and insufficient statistical power for this outcome. However, our data support the hypothesis that playing MDS when younger indeed enhances skeletal health—in our case, in females who ultimately became collegiate level cross-country runners.

RUN+MDS had enhanced whole-body and lumbar spine aBMD compared to RUN, with RUN having lower lumbar spine aBMD compared to reference data (i.e. z score < 0). The lower lumbar spine aBMD in RUN compared to reference data possibly reflects the systemic demands of distance running in terms of its impact on energy availability and circulating hormone levels. Twenty-one percent (3-out-of-14) of participants in our RUN group had low bone mass (i.e. a z score < -1), which matches the 19% reported by Tenforde et al. (31) in their similar cohort. In contrast, no participants in the MDS+RUN group had low bone mass. With equal number of participants in each group having possible low energy availability (i.e. LEAF-Q score = 8), the normalized lumbar spine aBMD to reference values in RUN+MDS and their greater whole-body aBMD compared to RUN suggests that MDS when younger helped facilitate general bone health. These data support those of Rauh et al. (19) who reported high school distance athletes who highly specialized in running (i.e. participation in distance running only and for ≥ 9 mth/yr) were 5 times more likely to have low aBMD compared to low sport specialists (≥ 1 nonrunning sport and distance-running sport/s for ≥ 8 mth/yr). Lower whole-body bone mass and lumbar spine aBMD have prospectively been shown to be predictive of BSI in female athletes (32).

Our HR-pQCT data at the distal tibia provides support for a benefit of MDS at a trabecular-rich site. The distal tibia in RUN+MDS had more trabecular bone (i.e. Tb.vBMD and Tb.BV/TV) with thicker trabeculae (i.e. Tb.Th) than RUN and enhanced cortical bone microarchitecture (i.e. Ct.Ar and Ct.Th). The enhanced bone microarchitecture in RUN+MDS cumulated in this group having 19.5% greater strength (i.e. failure load) at the distal tibia than RUN. The magnitude of strength enhancement in MDS-RUN is comparable to the 18.7% difference in distal radius bone strength observed between the racquet and non-racquet arms of collegiate level tennis players, a within-subject controlled model that minimizes the impact of inherited traits and systemic factors (24). Further supporting the benefit of MDS when young, MDS+RUN had greater Tt.vBMD, Tb.vBMD, Ct.Ar, Ct.Th, Tb.BV/TV, Tb.Th and failure load at the distal tibia compared to reference data (i.e. z score > 0) (28). No such differences were observed in RUN.

The distal tibia location assessed is not a site prone to BSI, although high-risk BSIs of the medial malleolus do occur nearby. When looking at more BSI-prone sites, we observed benefits of MDS at the diaphysis of both the 2nd MT and fibula. MT BSIs account for nearly one-quarter of BSIs in female collegiate cross-country runners and over one-third of all BSIs in collegiate athletes (17). Approximately 80% of MT BSIs occur in the 2nd and 3rd MTs (33) with bending strain during running estimated to be greatest in the 2nd MT compared to the other MTs (34, 35). Loading of the 2nd MT during stance principally occurs in the dorsal-plantar plane around a medial-lateral axis located toward the proximal end of the bone. The proximal location of the axis results from the proximal 2nd MT being relatively fixed in a mortise formed by the three cuneiforms and 1st and 3rd MTs. The fixation of the proximal 2nd MT creates a cantilever situation during stance to engender compression and tension on the dorsal and plantar surfaces of the diaphysis, respectively (36–39).

Loading of the 2nd MT during stance contributes to explaining the pattern of adaptation observed at the mid-diaphysis in RUN+MDS. The 2nd MT diaphysis in RUN+MDS was 10.4% larger (i.e. greater Tt.Ar), 19.9% thicker (i.e. greater Ct.Th), and had 23.3% greater

resistance to torsion (i.e. greater I_p) than in RUN. However, exploring the orthogonal axes of I_{MAX} and I_{MIN} , RUN+MDS had 32.5% greater I_{MAX} at the 2nd MT diaphysis than in RUN but there were no group differences in I_{MIN} . The I_{MAX} plane (or plane of greatest resistance to bending) within the diaphysis of the 2nd MT approximates the plantar-dorsal plane (40) and, thus, predominant adaptation in RUN+MDS appeared in the plane of greatest loading during stance. We did measure 18.6% greater failure load at the 2nd MT diaphysis in RUN+MDS, but this was to compressive loading along the bone's longitudinal axis and not to bending.

Similar to that observed at the 2nd MT, the fibula in RUN+MDS had 11.6% greater size (i.e. Tt.Ar) compared to in RUN. The fibula is the third most common site for BSI in collegiate level athletes after the tibia and metatarsals, accounting for 9.7% of all BSIs (17). The fibula carries less than 20% of the axial load applied to the leg (41), but is an important site for muscle attachment and muscle forces are the greatest contributor to bone loading (42, 43). Runners reportedly display limited adaptation at the fibula compared to controls, whereas soccer players exhibit enhanced fibular bone mass and geometry outcomes (44). The current data support that MDS may generate a more robust fibula that is more resistant to loading and subsequent BSI.

The greater Tt.Ar at both the 2nd MT and fibula diaphysis in RUN+MDS is of particular interest. Bone strength is proportional to the fourth power of material distance from the neutral axis. This means that small increases in bone size result in disproportionate increases in bone strength. Greater bone strength reduces tissue level stress and strain during each loading cycle to exponentially increase bone fatigue resistance (6). In terms of BSIs, bone geometry has been reported to be an important determinant of MT stress during loading (45) with enhanced geometric properties of the 2nd MT helping to normalize stresses in response to heightened external loads (38, 45, 46).

There is general consensus that most gains in bone size associated with mechanical loading are developed during the rapid modeling and periosteal bone apposition that occurs in the immature skeleton (3), although it is possible to influence bone size in skeletally mature individuals (47–50). The skeletal size changes induced when younger have the potential to persist long-term (5) and indicate that playing MDS during growth and delaying specialization in running are important to promote.

No differences were observed between groups at the tibial diaphysis, the most common site for BSI in female cross-country runners (17). This finding was unexpected as soccer and basketball players have been reported to have enhanced bone properties (12, 13) and reduced tibial strain per given load (14, 15). We have also shown multidirectional basketball activities load different regions of the tibial diaphysis (11) and used HR-pQCT to reveal dominant-to-nondominant leg differences at the tibial diaphysis in collegiate level tennis players (24). In the current study, RUN and RUN+MDS both had elevated Ct.Th at the tibial diaphysis compared to reference data (i.e. z score > 0), but that was the sole outcome showing differences. Ultimately, reasons for the absence of group differences at the tibial diaphysis are not known, but their absence provide support that the differences observed at

the other skeletal locations we assessed are true differences and not due to between-group differences in general skeletal properties caused by inherited traits and systemic factors.

The current study possesses several strengths, including the use of state-of-the-art HR-pQCT to provide measures of bone microarchitecture and micro-finite element estimated strength, recruitment of relatively comparable RUN and RUN+MDS groups in terms of BMI and potential presence of low energy availability, and inclusion of the radius as a control site. In terms of the latter, it is important to note that there were no differences between groups at either the distal radius or radial diaphysis indicating that differences observed at lower extremity sites were not due to globally elevated bone properties. The study also possesses limitations, including the use of a cross-sectional study design, non-study of males, relatively small sample size, modeling of micro-finite element estimated strength to axial compressive loading only, and use of physical activity recall to allocate participants to groups.

CONCLUSIONS

In summary, the current study found female cross-country runners who participated in MDS when younger had enhanced lower extremity bone size, microarchitecture, and strength compared to runners who solely ran (and swam or cycled). Group differences were observed at the distal tibia, common BSI sites (diaphyses of the fibula and 2nd MT) and select high-risk BSI sites (base of the 2nd MT, navicular, and proximal diaphysis of the 5th MT). However, no differences were observed at the tibial diaphysis. These data indicate that those supervising youth athletes should encourage a delay specialization in running and promote play in MDS, especially when younger, to build a more robust skeleton and potentially prevent BSIs. The current study focused on basketball and soccer but participation in other MDS, such as gymnastics, volleyball, and field hockey, may yield similar benefits.

Supplementary Material

Refer to Web version on PubMed Central for supplementary material.

Acknowledgements

This contribution was made possible by support from the National Institutes of Health (NIH/NIAMS P30 AR072581) and the Indiana Clinical Translational Science Award/Institute (NCATS UL1TR002529-01). The authors declare that they have no financial involvement or affiliations with any organizations or bodies with direct financial interest with the content discussed in this article. The results of the present study do not constitute endorsement by the American College of Sports Medicine. The results of this study are presented clearly, honestly, and without fabrication, falsification, or inappropriate data manipulation.

REFERENCES

1. Hoenig T, Ackerman KE, Beck BR, et al. Bone stress injuries. *Nat Rev Dis Primers*. 2022;8(1):26. [PubMed: 35484131]
2. Burr DB. Targeted and nontargeted remodeling. *Bone*. 2002;30(1):2–4. [PubMed: 11792556]
3. Warden SJ, Edwards WB, Willy RW. Preventing bone stress injuries in runners with optimal workload. *Curr Osteoporos Rep*. 2021;19(3):298–307. [PubMed: 33635519]
4. Edwards WB. Modeling overuse injuries in sport as a mechanical fatigue phenomenon. *Exerc Sport Sci Rev*. 2018;46(4):224–31. [PubMed: 30001271]

5. Warden SJ, Mantila Roosa SM, Kersh ME, et al. Physical activity when young provides lifelong benefits to cortical bone size and strength in men. *Proc Natl Acad Sci U S A*. 2014;111(14):5337–42. [PubMed: 24706816]
6. Warden SJ, Hurst JA, Sanders MS, Turner CH, Burr DB, Li J. Bone adaptation to a mechanical loading program significantly increases skeletal fatigue resistance. *J Bone Miner Res*. 2005;20(5):809–16. [PubMed: 15824854]
7. Fredericson M, Ngo J, Cobb K. Effects of ball sports on future risk of stress fracture in runners. *Clin J Sports Med*. 2005;15(3):136–41.
8. Milgrom C, Simkin A, Eldad A, Nyska M, Finestone A. Using bone's adaptation ability to lower the incidence of stress fractures. *Am J Sports Med*. 2000;28(2):245–51. [PubMed: 10751003]
9. Tenforde AS, Sayres LC, McCurdy ML, Sainani KL, Fredericson M. Identifying sex-specific risk factors for stress fractures in adolescent runners. *Med Sci Sports Exerc*. 2013;45(10):1843–51. [PubMed: 23584402]
10. Tenforde AS, Sainani KL, Carter Sayres L, Milgrom C, Fredericson M. Participation in ball sports may represent a prehabilitation strategy to prevent future stress fractures and promote bone health in young athletes. *PM R*. 2015;7(2):222–5. [PubMed: 25499072]
11. Yan C, Bice RJ, Frame JW, Warden SJ, Kersh ME. Multidirectional basketball activities load different regions of the tibia: a subject-specific muscle-driven finite element study. *Bone*. 2022;159:116392. [PubMed: 35314384]
12. Hughes JM, Dickin DC, Wang H. Soccer participation is associated with benefits in tibial bone cross-sectional geometry and strength in young women. *J Sports Med Phys Fitness*. 2022;62(7):969–73. [PubMed: 34498820]
13. Tenforde AS, Fredericson M. Influence of sports participation on bone health in the young athlete: a review of the literature. *PM R*. 2011;3(9):861–7. [PubMed: 21944303]
14. Hughes JM, Dickin DC, Wang H. The relationships between multiaxial loading history and tibial strains during load carriage. *J Sci Med Sport*. 2019;22(1):48–53. [PubMed: 29884594]
15. Wang H, Kia M, Dickin DC. Influences of load carriage and physical activity history on tibia bone strain. *J Sport Health Sci*. 2019;8(5):478–85. [PubMed: 31534823]
16. Changstrom BG, Brou L, Khodae M, Braund C, Comstock RD. Epidemiology of stress fracture injuries among US high school athletes, 2005–2006 through 2012–2013. *Am J Sports Med*. 2015;43(1):26–33. [PubMed: 25480834]
17. Rizzone KH, Ackerman KE, Roos KG, Dompier TP, Kerr ZY. The epidemiology of stress fractures in collegiate student-athletes, 2004–2005 through 2013–2014 academic years. *J Athl Train*. 2017;52(10):966–75. [PubMed: 28937802]
18. Barrack MT, Rauh MJ, Nichols JF. Prevalence of and traits associated with low BMD among female adolescent runners. *Med Sci Sports Exerc*. 2008;40(12):2015–21. [PubMed: 18981950]
19. Rauh MJ, Tenforde AS, Barrack MT, Rosenthal MD, Nichols JF. Sport specialization and low bone mineral density in female high school distance runners. *J Athl Train*. 2020;55(12):1239–46. [PubMed: 33176358]
20. Boden BP, Osbahr DC. High-risk stress fractures: evaluation and treatment. *J Am Acad Orthop Surg*. 2000;8(6):344–53. [PubMed: 11104398]
21. Bennell KL, Malcolm SA, Thomas SA, Wark JD, Brukner PD. The incidence and distribution of stress fractures in competitive track and field athletes. A twelve-month prospective study. *Am J Sports Med*. 1996;24(2):211–7. [PubMed: 8775123]
22. Proctor KL, Adams WC, Shaffrath JD, Van Loan MD. Upper-limb bone mineral density of female collegiate gymnasts versus controls. *Med Sci Sports Exerc*. 2002;34(11):1830–5. [PubMed: 12439090]
23. Melin A, Tornberg AB, Skouby S, et al. The LEAF questionnaire: a screening tool for the identification of female athletes at risk for the female athlete triad. *Br J Sports Med*. 2014;48(7):540–5. [PubMed: 24563388]
24. Warden SJ, Wright CS, Fuchs RK. Bone microarchitecture and strength adaptation to physical activity: a within-subject controlled, HRpQCT study. *Med Sci Sports Exerc*. 2021;53(6):1179–87. [PubMed: 33394902]

25. Bušková K, Bartoník J, Rammelt S. Fractures of the base of the fifth metatarsal bone: a critical analysis review. *JBJS Rev.* 2021;9(10):e21.00010.
26. Jepsen KJ, Evans R, Negus CH, et al. Variation in tibial functionality and fracture susceptibility among healthy, young adults arises from the acquisition of biologically distinct sets of traits. *J Bone Miner Res.* 2013;28(6):1290–300. [PubMed: 23362125]
27. Arias-Moreno AJ, Hosseini HS, Bevers M, Ito K, Zysset P, van Rietbergen B. Validation of distal radius failure load predictions by homogenized- and micro-finite element analyses based on second-generation high-resolution peripheral quantitative CT images. *Osteoporos Int.* 2019;30(7):1433–43. [PubMed: 30997546]
28. Warden SJ, Liu Z, Fuchs RK, van Rietbergen B, Moe SM. Reference data and calculators for second-generation HR-pQCT measures of the radius and tibia at anatomically standardized regions in White adults. *Osteoporos Int.* 2022;33(4):791–806. [PubMed: 34590158]
29. Yan C, Moshage SG, Kersh ME. Play during growth: the effect of sports on bone adaptation. *Curr Osteoporos Rep.* 2020;18(6):684–95. [PubMed: 33084999]
30. Rudolph SE, Caksa S, Gehman S, et al. Physical activity, menstrual history, and bone microarchitecture in female athletes with multiple bone stress injuries. *Med Sci Sports Exerc.* 2021;53(10):2182–9. [PubMed: 33831898]
31. Tenforde AS, Carlson JL, Sainani KL, et al. Sport and triad risk factors influence bone mineral density in collegiate athletes. *Med Sci Sports Exerc.* 2018;50(12):2536–43. [PubMed: 29975299]
32. Bennell KL, Malcolm SA, Thomas SA, et al. Risk factors for stress fractures in track and field athletes: a twelve-month prospective study. *Am J Sports Med.* 1996;24(6):810–8. [PubMed: 8947404]
33. Fetzer GB, Wright RW. Metatarsal shaft fractures and fractures of the proximal fifth metatarsal. *Clin Sports Med.* 2006;25(1):139–50. [PubMed: 16324980]
34. Donahue SW, Sharkey NA. Strains in the metatarsals during the stance phases of gait: implications for stress fractures. *J Bone Joint Surg Am.* 1999;81(9):1236–44. [PubMed: 10505520]
35. Gross TS, Bunch RP. A mechanical model of metatarsal stress fracture during distance running. *Am J Sports Med.* 1989;17(5):669–74. [PubMed: 2610283]
36. Arndt A, Ekenman I, Westblad P, Lundberg A. Effects of fatigue and load variation on metatarsal deformation measured in vivo during barefoot walking. *J Biomech.* 2002;35(5):621–8. [PubMed: 11955501]
37. Ellison MA, Akrami M, Fulford J, Javadi AA, Rice HM. Three dimensional finite element modelling of metatarsal stresses during running. *J Med Eng Technol.* 2020;44(7):368–77. [PubMed: 32762585]
38. Ellison MA, Kenny M, Fulford J, Javadi A, Rice HM. Incorporating subject-specific geometry to compare metatarsal stress during running with different foot strike patterns. *J Biomech.* 2020;105:109792. [PubMed: 32327192]
39. Firminger CR, Fung A, Loundagin LL, Edwards WB. Effects of footwear and stride length on metatarsal strains and failure in running. *Clin Biomech.* 2017;49:8–15.
40. Muehleman C, Lidtke R, Berzins A, Becker JH, Shott S, Sumner DR. Contributions of bone density and geometry to the strength of the human second metatarsal. *Bone.* 2000;27(5):709–14. [PubMed: 11062360]
41. Wang Q, Whittle M, Cunningham J, Kenwright J. Fibula and its ligaments in load transmission and ankle joint stability. *Clin Orthop Relat Res.* 1996(330):261–70.
42. Avin KG, Bloomfield SA, Gross TS, Warden SJ. Biomechanical aspects of the muscle-bone interaction. *Curr Osteoporos Rep.* 2015;13(1):1–8. [PubMed: 25515697]
43. Matijevich ES, Branscombe LM, Scott LR, Zelik KE. Ground reaction force metrics are not strongly correlated with tibial bone load when running across speeds and slopes: implications for science, sport and wearable tech. *PLoS One.* 2019;14(1):e0210000. [PubMed: 30653510]
44. Rittweger J, Ireland A, Lüscher S, et al. Fibula: the forgotten bone—may it provide some insight on a wider scope for bone mechanostat control? *Curr Osteoporos Rep.* 2018;16(6):775–8. [PubMed: 30393831]
45. Nunns M, Stiles V, Fulford J, Dixon S. Estimated third metatarsal bending stresses are highly susceptible to variations in bone geometry. *Footwear Sci.* 2017;9(3):127–37.

46. Ellison MA, Fulford J, Javadi A, Rice HM. Do non-rearfoot runners experience greater second metatarsal stresses than rearfoot runners? *J Biomech.* 2021;126:110647. [PubMed: 34343863]
47. Eleftheriou KI, Rawal JS, Kehoe A, et al. The Lichfield bone study: the skeletal response to exercise in healthy young men. *J Appl Physiol (1985).* 2012;112(4):615–26. [PubMed: 22114178]
48. Izard RM, Fraser WD, Negus C, Sale C, Greeves JP. Increased density and periosteal expansion of the tibia in young adult men following short-term arduous training. *Bone.* 2016;88:13–9. [PubMed: 27046087]
49. O’Leary TJ, Izard RM, Tang JCY, Fraser WD, Greeves JP. Sex differences in tibial adaptations to arduous training: an observational cohort study. *Bone.* 2022;160:116426. [PubMed: 35470123]
50. O’Leary TJ, Izard RM, Walsh NP, Tang JCY, Fraser WD, Greeves JP. Skeletal macro- and microstructure adaptations in men undergoing arduous military training. *Bone.* 2019;125:54–60. [PubMed: 31077851]

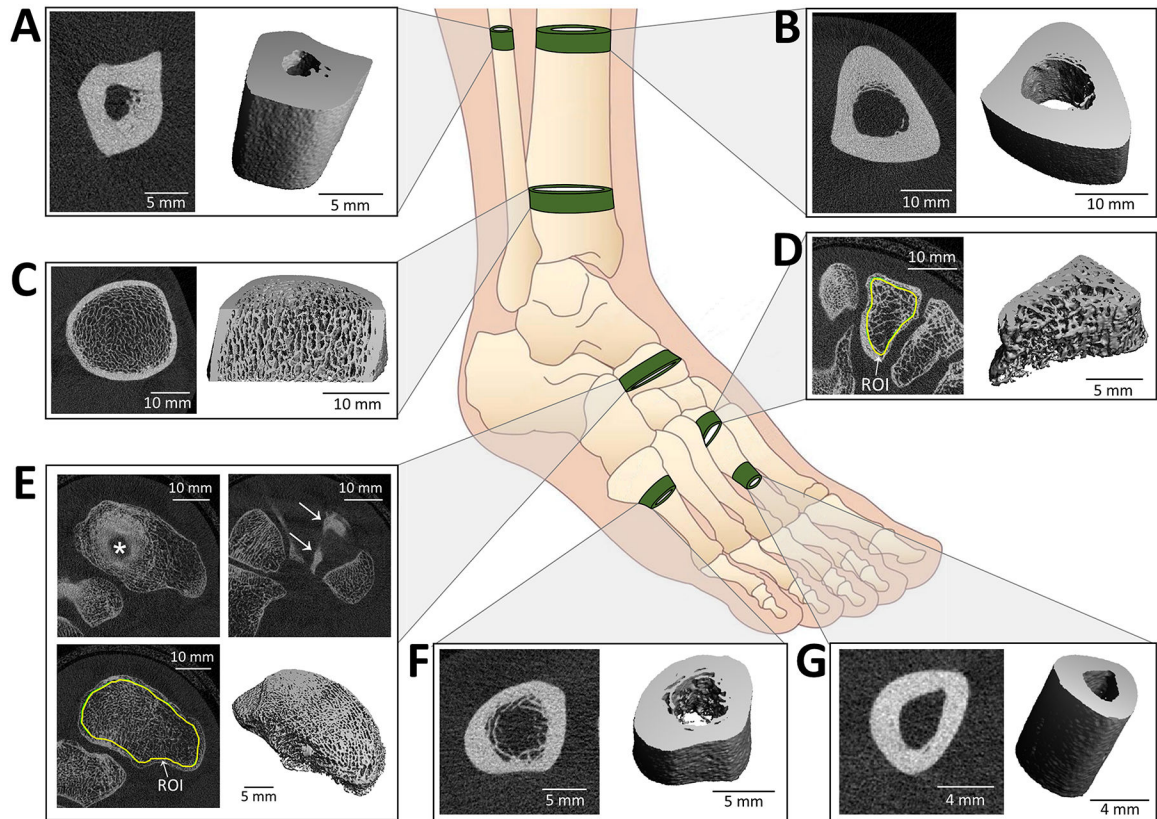


Fig. 1.

Skeletal sites of interest were the fibular (A) and tibial diaphysis (B), distal tibia (C), base of the 2nd MT (D), navicular (E), proximal diaphysis of the 5th MT (F) and 2nd MT diaphysis (G). In each panel, the left image shows a representative HR-pQCT slice at the site of interest. The image on the right in each panel shows a representative 3D reconstruction of the analyzed slices. In panel E, the top two images show the slices identifying the floor of the navicular facet (*) and ridges on the distal navicular at the navicular-cuneiform complex (arrows). These landmarks were used to define the volume of interest. In panels D and E, the region of interest (ROI) manually traced inside the cortical shell is shown in the HR-pQCT slice.

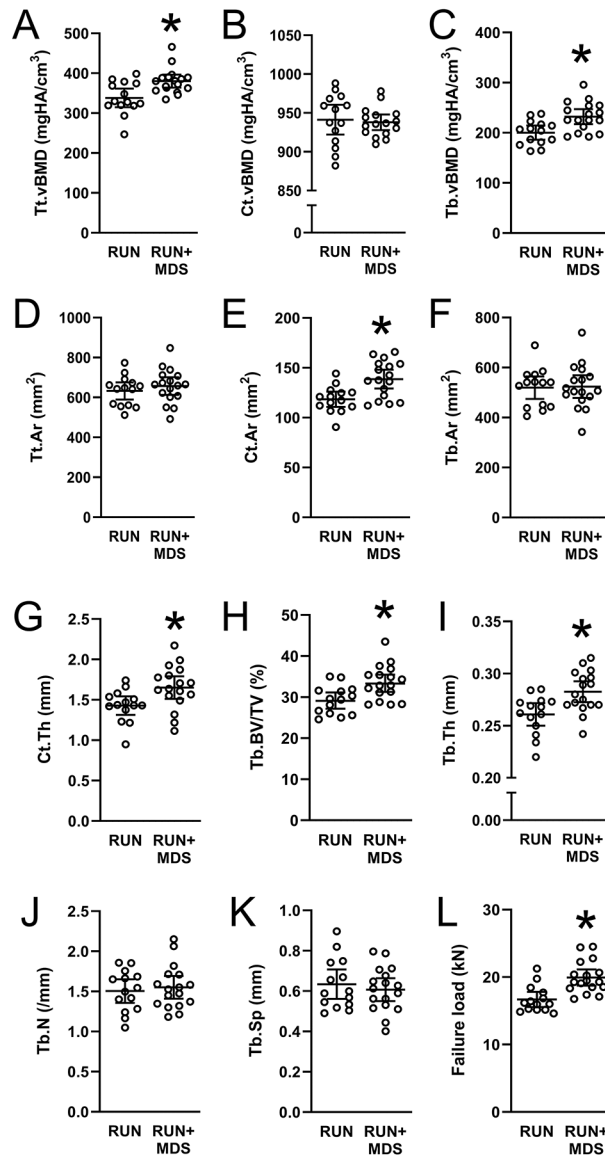


Fig. 2. Distal tibia properties in RUN and RUN+MDS. A) Total volumetric bone mineral density [Tt.vBMD]; B) cortical vBMD [Ct.vBMD]; C) trabecular vBMD [Tb.vBMD]; D) total area [Tt.Ar]; E) cortical area [Ct.Ar]; F) trabecular area [Tb.Ar]; G) cortical thickness [Ct.Th]; H) trabecular bone volume/tissue volume [Tb.BV/TV]; I) trabecular thickness [Tb.Th]; J) trabecular number [Tb.N]; K) trabecular spacing [Tb.Sp], and; L) failure load. Mean \pm 95% confidence interval and individual participant data (open circles) are shown. * $p < 0.05$ between groups.

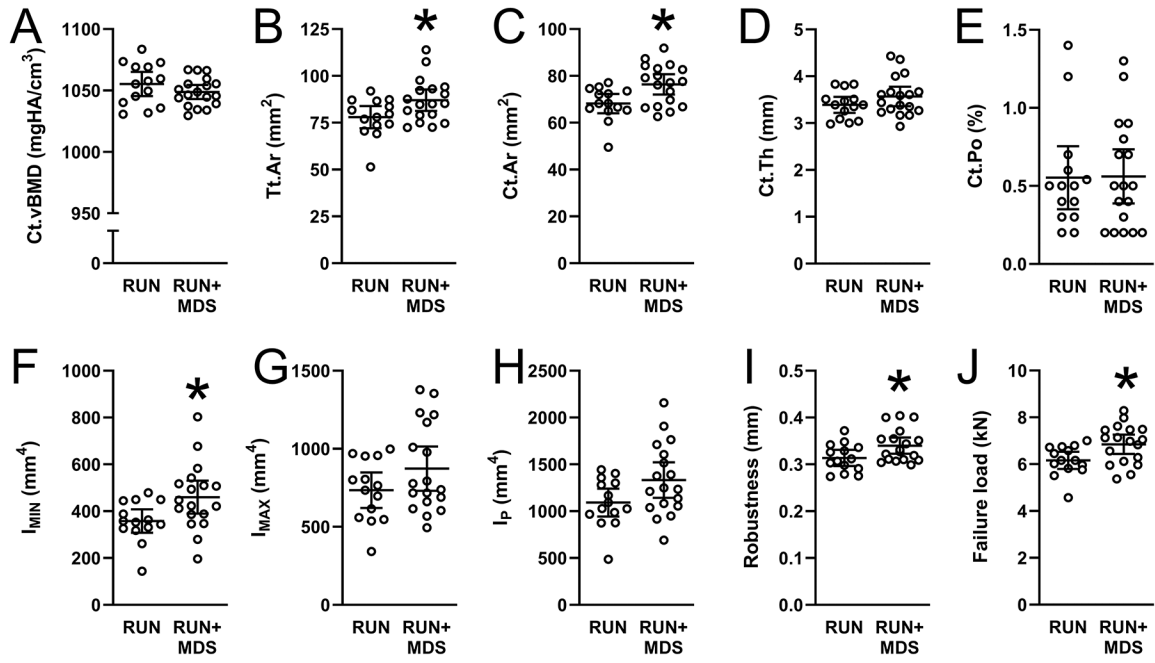


Fig. 3. Fibula diaphysis properties in RUN and RUN+MDS. A) Cortical volumetric bone mineral density [Ct.vBMD]; B) total area [Tt.Ar]; C) cortical area [Ct.Ar]; D) cortical thickness [Ct.Th]; E) cortical porosity [Ct.Po]; F) minimum second moment of area [I_{MIN}]; G) maximum second moment of area [I_{MAX}]; H) polar moment of inertia [I_P]; I) robustness, and; J) failure load. Mean ± 95% confidence interval and individual participant data (open circles) are shown. * $p < 0.05$ between groups.

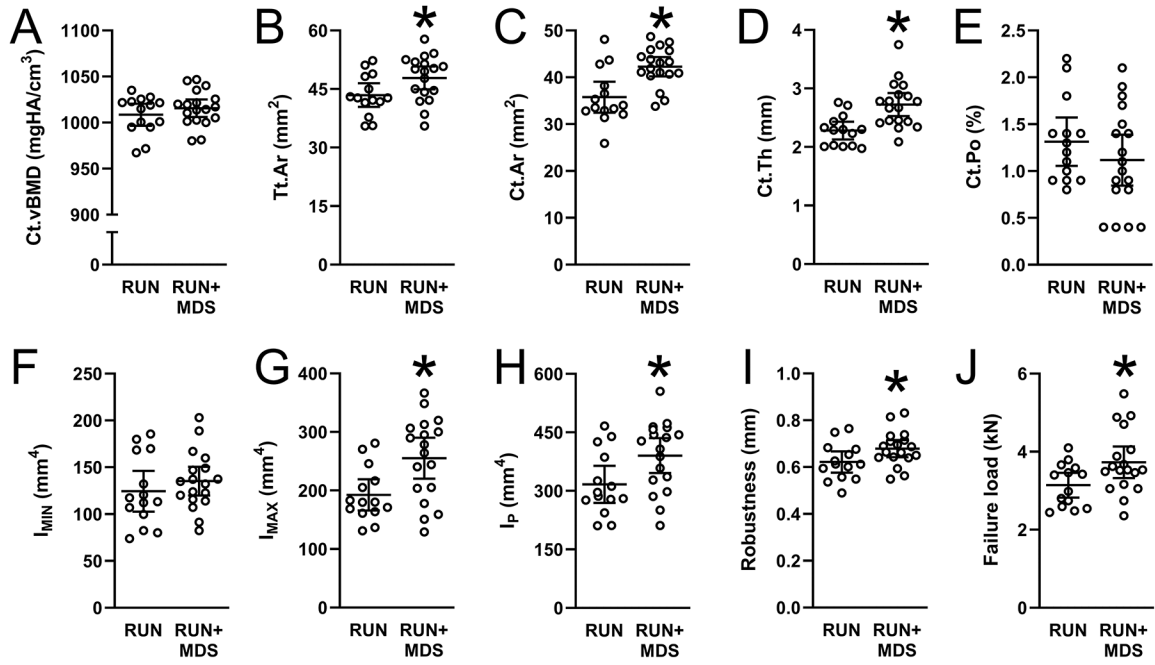


Fig. 4. Properties of the 2nd MT diaphysis in RUN and RUN+MDS. A) Cortical volumetric bone mineral density [Ct.vBMD]; B) total area [Tt.Ar]; C) cortical area [Ct.Ar]; D) cortical thickness [Ct.Th]; E) cortical porosity [Ct.Po]; F) minimum second moment of area [I_{MIN}]; G) maximum second moment of area [I_{MAX}]; H) polar moment of inertia [I_P]; I) robustness, and; J) failure load. Mean ± 95% confidence interval and individual participant data (open circles) are shown. **p*<0.05 between groups.

Table 1.Participant characteristics^a

Characteristic	RUN	RUN+MDS	P value
Demographics			
<i>n</i>	14	18	
Age (yrs)	21.0 ± 1.6	20.6 ± 1.6	0.46
BSI history (no/yes)	5 / 9	10 / 8	0.26
BSIs per athlete (<i>n</i>)	1.4 ± 1.7	0.7 ± 0.8	0.14
Age of menarche (yr)	13.5 ± 1.7	13.3 ± 1.5	0.77
LEAF-Q score	7.3 ± 4.2	7.3 ± 5.0	0.99
LEAF-Q score < 8 (yes/no)	7 / 7	7 / 11	0.40
<9 menstrual cycles in past year (yes/no)	3 / 11	3 / 15	0.73
Past history of menstrual dysfunction >3 mths (yes/no)	5 / 9	9 / 9	0.42
Age started cross country (yr)	11.2 ± 1.7	11.7 ± 2.8	0.60
Total years of cross country (yr)	9.8 ± 2.3	8.9 ± 3.0	0.38
Best cross country 5 km time (mm:ss)	18:34 ± 00:38	18:21 ± 00:47	0.46
Age started MDS (yr)	—	5.8 ± 1.9	—
Years playing MDS before menarche (yr)	—	7.7 ± 2.4	—
Total years played MDS (yr)	—	10.3 ± 3.2	—
Whole-body anthropometry			
Height (m)	1.65 ± 0.06	1.67 ± 0.06	0.36
Mass (kg)	57.0 ± 4.2	59.9 ± 5.4	0.10
Body mass index (kg/m ²)	20.9 ± 1.6	21.4 ± 1.9	0.39
Whole-body aBMD (g/cm ²) ^b	0.890 ± 0.041	0.942 ± 0.072	0.02*
Whole-body aBMD z score	-0.30 (-0.67 to 0.08)	0.09 (-0.37 to 0.55)	
Lean mass (kg)	39.3 ± 4.1	41.7 ± 3.6	0.09
Fat mass (%)	21.2 ± 5.1	21.5 ± 4.3	0.84
Regional anthropometry			
Lumbar spine aBMD (g/cm ²) ^b	1.015 ± 0.110	1.096 ± 0.128	0.05*
Lumbar spine aBMD z score	-0.45 (-0.85 to -0.04) [†]	0.18 (-0.23 to 0.58)	
Hip aBMD (g/cm ²) ^b	1.095 ± 0.091	1.138 ± 0.129	0.31
Hip aBMD z score	1.06 (0.62 to 1.50) [†]	1.60 (1.14 to 2.07) [†]	
Distal radius HRpQCT outcomes^c			
Cortical thickness (mm) ^d	0.88 ± 0.16	0.91 ± 0.13	0.56
Cortical thickness z score	0.09 (-0.53 to 0.72)	0.30 (-0.15 to 0.75)	
Trabecular BV/TV (%) ^b	23.1 ± 4.4	24.8 ± 4.7	0.31
Trabecular BV/TV z score	-0.05 (-0.58 to 0.49)	0.29 (-0.21 to 0.80)	
Failure load (kN) ^d	5.33 ± 0.73	5.83 ± 1.04	0.14
Failure load z score	-0.21 (-0.56 to 0.13)	0.28 (-0.22 to 0.78)	

Characteristic	RUN	RUN+MDS	P value
Radial diaphysis HRpQCT outcomes^e			
Total area (mm ²) ^d	86.9 ± 8.1	89.3 ± 10.2	0.47
Total area z score	-0.33 (-0.70 to 0.05)	-0.16 (-0.55 to 0.23)	
Cortical thickness (mm) ^d	3.19 ± 0.25	3.33 ± 0.24	0.13
Cortical thickness z score	-0.34 (-0.86 to 0.18)	0.15 (-0.28 to 0.58)	
Polar moment of inertia (mm ⁴) ^{d,f}	1246 ± 168	1334 ± 303	0.34

aBMD = areal bone mineral density; BSI = bone stress injury; BV/TV = bone volume per tissue volume; HRpQCT = high-resolution peripheral quantitative computed tomography; LEAF-Q = Low Energy Availability in Females Questionnaire; MDS = multidirectional sport

^aData are mean ± SD, except for BSI history and LEAF-Q score [8 [frequencies] and z scores [mean (95% confidence interval)]]

^bValues adjusted for LEAF-Q score and whole-body lean mass

^cSelect outcomes at the distal radius. See Supplementary figures 1 & 2 for full data

^dValues adjusted for LEAF-Q score, whole-body lean mass, and bone length

^eSelect outcomes at the radial diaphysis. See Supplementary figures 3 & 4 for full data

^fNormative reference data for this outcome is not available

* Significant difference between groups ($p < 0.05$)

† Confidence interval does not cross zero

Table 2.HRpQCT properties at selected high risk BSI sites in RUN and RUN+MDS^a

Skeletal site and outcome	RUN	RUN+MDS	P value
Base of the 2nd metatarsal			
Trabecular bone volume per tissue volume (%) ^b	40.3 ± 5.2	43.6 ± 4.9	0.09
Trabecular thickness (mm) ^b	0.282 ± 0.010	0.298 ± 0.020	0.02 *
Trabecular number (1/mm) ^b	1.81 ± 0.22	1.84 ± 0.20	0.68
Trabecular spacing (mm) ^b	0.557 ± 0.087	0.561 ± 0.067	0.91
Navicular			
Trabecular bone volume per tissue volume (%) ^b	38.0 ± 2.7	41.1 ± 4.1	0.01 *
Trabecular thickness (mm) ^b	0.299 ± 0.030	0.329 ± 0.031	0.01 *
Trabecular number (1/mm) ^b	1.87 ± 0.21	1.85 ± 0.18	0.79
Trabecular spacing (mm) ^b	0.498 ± 0.055	0.502 ± 0.054	0.84
Proximal diaphysis of the 5th metatarsal			
Cortical vBMD (mgHA/cm ³)	947 ± 25	956 ± 25	0.36
Total area (mm ²) ^c	74.5 ± 8.3	79.3 ± 8.3	0.13
Cortical area (mm ²) ^c	49.9 ± 5.8	55.3 ± 4.7	<0.01 *
Cortical thickness (mm) ^c	2.21 ± 0.25	2.47 ± 0.33	0.02 *
Cortical porosity (%)	2.37 ± 0.73	2.07 ± 1.09	0.41
Minimum second moment of inertia (mm ⁴) ^c	258 ± 49	293 ± 58	0.08
Maximum second moment of inertia (mm ⁴) ^c	625 ± 159	721 ± 149	0.09
Polar moment of inertia (mm ⁴) ^c	883 ± 195	1014 ± 189	0.06

^aData are mean ± SD^bValues adjusted for LEAF-Q score and whole-body lean mass^cValues adjusted for LEAF-Q score, whole-body lean mass, and bone length